Inerter Effects for Running Robots with Mechanical Impedance

Yuta Hanazawa[1], Rin Takano[2] and Masaki Yamakita[2]

***Abstract*— This paper presents inerer effect for achieving high-speed running of legged robots. The previous simplest biped robot with mechanical impedance consisted of a mass and a telescopic leg with a spring. However, the running speed of the robot is limited by the natural period of the model, which cannot be freely designed. Our proposed method overcomes this limitation by virtue of the inerter. The effectiveness of the proposed method is demonstrated through a mathematical analysis and numerical simulations.**

I. INTRODUCTION

Recently biped robots achieve stable dynamic walking [1], [2]. Many researchers have concentrated on Zero Moment Point (ZMP) based control biped robots, which achieves relatively fast running speeds [1], [3], [4]. However, the current generation of robots cannot reach human running speeds, and the achievement of faster than human running speeds remains a challenging task. When we consider model of the running robot, we deal with the simple telescopic leg robot with spring [5], [6], [7], [8], [9]. One legged robot with the spring was developed as a simple running robot based on human and animal running [10], [11], [12], [13]. This robot model is a convenient tool for running analysis and is used in the design of running control methods.

To achieve high-speed running by the robot, we require appropriate dynamics of the robot. The running speed depends on the angle of the leg from the vertical line at the lift-off (LO). Fig. 1 illustrates slow and fast running in the robot. Slow and fast running speeds are obtained by shortening and the lengthening the step length, respectively. To accelerate the running, the LO timing is delayed by the robot dynamics.

The LO timing depends on the natural period of the robot imposed by the mass and spring. However, as the amplitude of the leg length during running also depends on the mass and spring, we cannot freely design the natural period of the robot. Therefore, the robot cannot attain very fast running speeds.

To resolve the above problem, we propose a robot for high-speed running robots with the inerter. The inerter is a mechanical element that treats inertia as a mechanical impedance [14]. It is constructed from gears and a flywheel and the inertia is altered by changing the gear ratio and the flywheel inertia. Through the inerter, we can freely design the natural period of the robot. We expect that increasing the natural period of the robot will increase its running speed. In this paper, we analytically study the simplest robot with the inerter and confirm its effectiveness through numerical simulations.

[1]Y. Hanazawa is with the Dept. of Applied Science for Integrated System Engineering, Graduate School of Engineering, Kyushu Institute of Technology, 1-1 Sensui, Tobata, Kitakyushu, Fukuoka 804-8550, JAPAN hanazawa-y@ise.kyutech.ac.jp [2]R. Takano and M. Yamakita are with the Dept. of Mechanical and Control Engineering, Tokyo Institute of Technology, 2-12-1 Oh-okayama, Meguro-ku Tokyo 152-8552, JAPAN {takano, yamakita}@ac.ctrl.titech.ac.jp

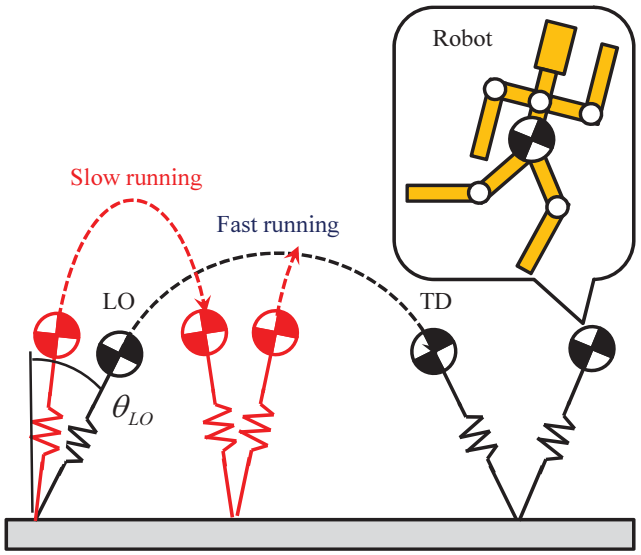

Fig. 1. Schematic of slow and fast running in the simplest running robot

II. MODEL OF ROBOT

A. Dynamic Equation

The proposed model is schematized in Fig. 2. The robot performs passive dynamic walking [15] on a slope. The robot is constructed from a flywheel body, an actuator, and a telescopic-leg with a spring and inerter.

The dynamic equation of the robot is given by

$$\boldsymbol{M}(\boldsymbol{q})\ddot{\boldsymbol{q}} + \boldsymbol{H}(\boldsymbol{q}, \dot{\boldsymbol{q}}) = \boldsymbol{S}(\boldsymbol{u} + \boldsymbol{\tau}_K + \boldsymbol{\tau}_B) + \boldsymbol{J}_c^{\mathrm{T}}\boldsymbol{\lambda}, \quad (1)$$

where $\boldsymbol{q} = [\theta_1,\ \theta_2,\ l_1,\ x_1,\ z_1]^{\mathrm{T}}$is the generalized coordinate vector, $\boldsymbol{M}(\boldsymbol{q}) \in \mathbb{R}^{5\times5}$ is the inertia matrix, $\boldsymbol{H}(\boldsymbol{q}, \dot{\boldsymbol{q}}) \in \mathbb{R}^5$ is a vector comprising the Coriolis force, centrifugal force, and gravitational vector, and $\boldsymbol{u} = [u_1,\ 0]^{\mathrm{T}}$ is the input vector, $\boldsymbol{\tau}_K = [0,\ f_K]^{\mathrm{T}}$ and $\boldsymbol{\tau}_B = [0,\ f_B]^{\mathrm{T}}$ are the force vectors associated with the spring of the leg, and the inerter of the leg, respectively. $\boldsymbol{S} \in \mathbb{R}^{5\times2}$ is the following driving matrix:

$$\boldsymbol{S} = \begin{bmatrix} -1 & 0 \\ 1 & 0 \\ 0 & 1 \\ 0 & 0 \\ 0 & 0 \end{bmatrix}.$$

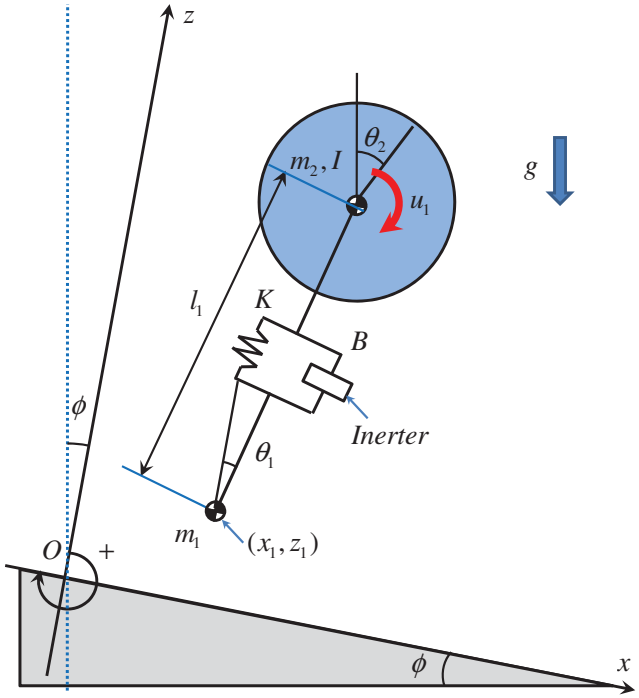

Fig. 2. Running model with mechanical impedance on a slope. The mechanical impedance components are with a spring (with spring constant K) and inerter (with inerter constant B)

The force due to the spring is given by

$$f_K = -K(l_1 - l_0), \tag{2}$$

where K [N/m] is the spring constant. The force due to the inerter is given by

$$f_B = -B\ddot{l_1}, \tag{3}$$

where B [N/(m/s^2)] is the inerter constant. We transform the dynamic equation,

$$\boldsymbol{M}_B(\boldsymbol{q})\ddot{\boldsymbol{q}} + \boldsymbol{H}(\boldsymbol{q}, \dot{\boldsymbol{q}}) = \boldsymbol{S}(\boldsymbol{u} + \boldsymbol{\tau}_K) + \boldsymbol{J}_c^{\mathrm{T}}\boldsymbol{\lambda}, \tag{4}$$

where the new inertia matrix $\boldsymbol{M}_B(\boldsymbol{q})$ comprises $\boldsymbol{M}(\boldsymbol{q})$ and the inertia imposed by the inerter. Here the third-row third-column element in $\boldsymbol{M}_B(\boldsymbol{q})$ is given by

$$M_{B33} = M_{33} + B, \tag{5}$$

where M_{33} is the third-row third-column element in $\boldsymbol{M}(\boldsymbol{q})$. Therefore, the inerter changes only the inertia matrix without changing the gravitational vector.

$\boldsymbol{J}_c \in \mathbb{R}^{N\times 5}$ is the Jacobian matrix, determined under the N constraint conditions of the robot. The constraint force vector $\boldsymbol{\lambda} \in \mathbb{R}^N$ is given by

$$\boldsymbol{\lambda} = -\boldsymbol{X}(\boldsymbol{q})^{-1}(\boldsymbol{J}_c\boldsymbol{M}_B(\boldsymbol{q})^{-1}\boldsymbol{\Gamma}(\boldsymbol{q},\dot{\boldsymbol{q}},\boldsymbol{u}) + \dot{\boldsymbol{J}}_c\dot{\boldsymbol{q}}), \tag{6}$$

where

$$\boldsymbol{X}(\boldsymbol{q}) = \boldsymbol{J}_c\boldsymbol{M}_B(\boldsymbol{q})^{-1}\boldsymbol{J}_c^{\mathrm{T}}, \tag{7}$$

$$\boldsymbol{\Gamma}(\boldsymbol{q}, \dot{\boldsymbol{q}}, \boldsymbol{u}) = \boldsymbol{S}(\boldsymbol{u} + \boldsymbol{\tau}_K) - \boldsymbol{H}(\boldsymbol{q}, \dot{\boldsymbol{q}}). \tag{8}$$

B. Constraint Conditions of the Robot

Running changes the contact conditions in our model. The contact phase is assumed as the contact period of the leg-tip with the ground, and flight phase occurs when the leg leaves the ground. In the contact phase, the leg-tip is constrained on the ground, and the constraint equations are given by

$$\dot{x}_1 = 0, \tag{9}$$

$$\dot{z}_1 = 0. \tag{10}$$

From these equations, $\boldsymbol{J}_c \in \mathbb{R}^{2\times 5}$ and $\dot{\boldsymbol{J}}_{\boldsymbol{c}} \in \mathbb{R}^{2\times 5}$ are obtained as

$$\boldsymbol{J}_c\dot{\boldsymbol{q}} = \begin{bmatrix} 0 & 0 & 0 & 1 & 0 \\ 0 & 0 & 0 & 0 & 1 \end{bmatrix}\dot{\boldsymbol{q}} = \boldsymbol{0}_{2\times 1}, \tag{11}$$

$$\dot{\boldsymbol{J}}_c = \boldsymbol{0}_{2\times 5}. \tag{12}$$

C. Generated LO Condition

During running, LO transitions the dynamics from contact phase to flight phase. LO is assumed to be generated by zero of the ground reaction force of the leg-tip. The LO condition is then given by

$$F_z = 0, \tag{13}$$

where F_z is the vertical elements of the constraint force at the leg-tip. When Eq. (13) is satisfied, we set $\lambda = 0$ in Eq. (4).

D. Impact Equation

Leg collisions with ground are assumed to be inelastic and instantaneous. The velocity of the robot immediately after a collision is obtained by impact equation [16]. When the leg-tip touches the ground, the constraint equation $\boldsymbol{J}_I \in \mathbb{R}^{2\times 5}$ of the robot is given by

$$\boldsymbol{J}_I\dot{\boldsymbol{q}} = \begin{bmatrix} 0 & 0 & 0 & 1 & 0 \\ 0 & 0 & 0 & 0 & 1 \end{bmatrix}\dot{\boldsymbol{q}} = \boldsymbol{0}_{2\times 1}. \tag{14}$$

The impulse vector, $\boldsymbol{\lambda}_I \in \mathbb{R}^2$ and the velocity vector immediately after impact, $\dot{\boldsymbol{q}}^+ \in \mathbb{R}^5$ are respectively given by

$$\boldsymbol{\lambda}_I = -\boldsymbol{X}_I(\boldsymbol{q})^{-1}\boldsymbol{J}_I\dot{\boldsymbol{q}}^-, \tag{15}$$

$$\dot{\boldsymbol{q}}^+ = (\boldsymbol{I}_5 - \boldsymbol{M}_B(\boldsymbol{q})^{-1}\boldsymbol{J}_I^{\mathrm{T}}\boldsymbol{X}_I(\boldsymbol{q})^{-1}\boldsymbol{J}_I)\dot{\boldsymbol{q}}^-, \tag{16}$$

where $\boldsymbol{X}_I(\boldsymbol{q}) := \boldsymbol{J}_I\boldsymbol{M}_B(\boldsymbol{q})^{-1}\boldsymbol{J}_I^{\mathrm{T}}$ and $\dot{\boldsymbol{q}}^- \in \mathbb{R}^5$ is the velocity immediately before impact.

III. CONTROL METHODS

The input to the contact phase is given by

$$u_1 = -K_{P1}\theta_2 - K_{D1}\dot{\theta}_2, \tag{17}$$

where K_{P1}, K_{D1} are the control gains. This input achieves a vertical torso angle. The input to the flight phase is then given by

$$u_1 = -K_{P2}(\theta_1 - \alpha) - K_{D2}\dot{\theta}_1, \tag{18}$$

where K_{P2}, K_{D2} are the control gains, and α is the desired leg angle. This input ensures a leg angle of α in the flight phase.

As the ideal 1-periodic running trajectory, we assume a symmetrical running trajectory. More specifically, the leg angle at touch down (TD) and LO are symmetrical about the vertical line, as expressed in the following equation:

$$-\theta^i_{TD} = \theta^i_{LO} = -\theta^{i+1}_{TD} = \theta^{i+1}_{LO}. \tag{19}$$

The leg angle α governed by the control method should satisfy Eq. (19) as far as possible. Fig. 3 is a schematic of the control method. The black and red solid lines show the actual and ideal leg postures during TD and LO, respectively, at the i-th step. The ideal leg postures are symmetric about the middle point of c defined as the distance between the mass points at the TD and LO:

$$c = l^i_{TD}\sin(-\theta^i_{TD}) + l^i_{LO}\sin\theta^i_{LO}. \tag{20}$$

We then assumed that the length of the robot's leg is the natural length L at the desired posture. The desired leg angle α is then given by

$$\alpha = -\sin^{-1}\Big(\frac{c}{2L}\Big). \tag{21}$$

IV. Analysis of Translational Motion in Contact Phase

To validate the effectiveness of the inerter, we analyze the translational motion in the contact phase. For simplicity, we consider the model with a spring, damper and inerter similar to the robot vertically fixed on the ground as shown in Fig. 4. The dynamic equation is given by

$$M_1\ddot{z} = -K_1 z - D_1\dot{z} - B_1\ddot{z} - M_1 g, \tag{22}$$

Rearranging Eq. (22), we obtain

$$\ddot{z} + 2\zeta\omega_n\dot{z} + \omega_n^2 z = -F. \tag{23}$$

where $2\zeta\omega_n = D_1/M_I$, $\omega_n^2 = K_1/M_I$, $F = M_1 g/M_I$, and $M_I = M_1 + B_1$.

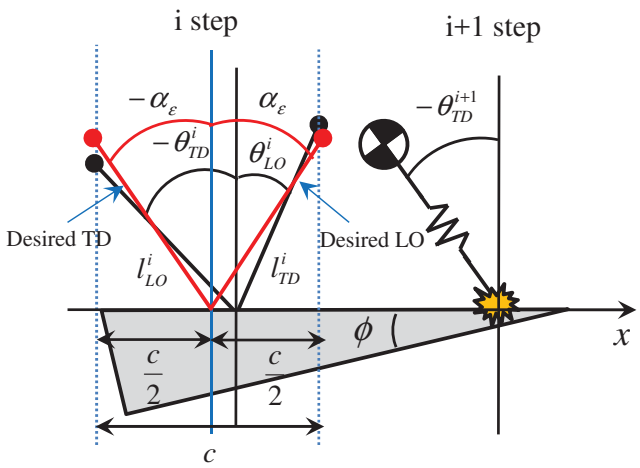

Fig. 3. Schematic of the control method

Taking the Laplace transform of Eq. (23) and setting the initial value as $z(0) = \dot{z}(0) = 0$, we get the following equation:

$$s^2 Z(s) + 2\zeta\omega_n s Z(s) + \omega_n^2 Z(s) = -\frac{F}{s}. \tag{24}$$

Eq. (24) then transforms as

$$\begin{aligned} Z(s) &= -F\Big(\frac{1}{\omega_n^2}\frac{1}{s} - \frac{\frac{1}{\omega_n^2}s + 2\frac{\zeta}{\omega_n}}{s^2 + 2\zeta\omega_n s + \omega_n^2}\Big), \\ &= -\frac{F}{\omega_n^2}\Big(\frac{1}{s} - \frac{s + 2\zeta\omega_n}{(s+\zeta\omega_n)^2 - \zeta^2\omega_n^2 + \omega_n^2}\Big), \\ &= -\frac{F}{\omega_n^2}\Big(\frac{1}{s} - \Big(\frac{s+\zeta\omega_n}{(s+\zeta\omega_n)^2 + \omega_d^2} \\ &\qquad + \frac{\zeta\omega_n}{(s+\zeta\omega_n)^2 + \omega_d^2}\Big)\Big), \end{aligned} \tag{25}$$

where $\omega_d = \omega_n\sqrt{1-\zeta^2}$.

Taking the inverse Laplace transformation of Eq. (25), we get

$$\begin{aligned} z &= -\frac{F}{\omega_n^2}\Big(1 - \Big(e^{-\zeta\omega_n t}\cos\omega_d t + \frac{\zeta\omega_n}{\omega_d}e^{-\zeta\omega_n t}\sin\omega_d t\Big)\Big), \\ &= -\frac{F}{\omega_n^2}\Big(1 - e^{-\zeta\omega_n t}\frac{1}{\sqrt{1-\zeta^2}}\sin(\omega_d t + \psi)\Big), \end{aligned} \tag{26}$$

where $\psi = \tan^{-1}(\sqrt{1-\zeta^2}/\zeta)$.

For simplicity, we assumed that the viscosity constant D_1 of the damper is negligibly small. From $F = M_1 g/M_I$ and $\omega_n = \sqrt{K_1/(M_1 + B_1)}$, we get

$$z = -\frac{M_1}{K_1}g\Big(1 - \sin\Big(\sqrt{\frac{K_1}{M_1 + B_1}}t + \pi/2\Big)\Big). \tag{27}$$

The parameters M_1 and K_1 determine the amplitude and natural frequency of the robot leg, respectively. The natural frequency additionally depends on B_1. Therefore, the inerter allows free design of the natural period ($T_n = 2\pi/\omega_n$).

Using simple examples, we now show the effectiveness of the inerter of the model. The natural period of the motion

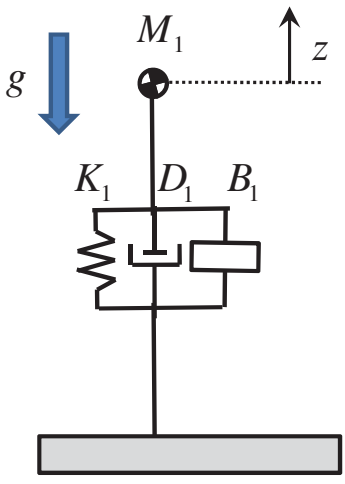

Fig. 4. Translational analysis of a spring, damper, and ineter model with a vertically fixed posture

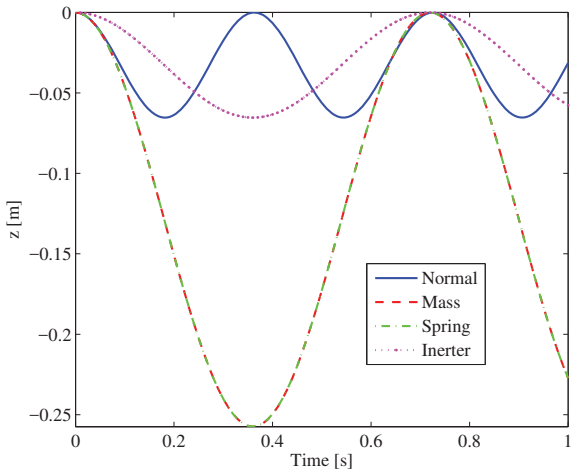

Fig. 5. Telescopic motions of the model under four conditions in the translational analysis

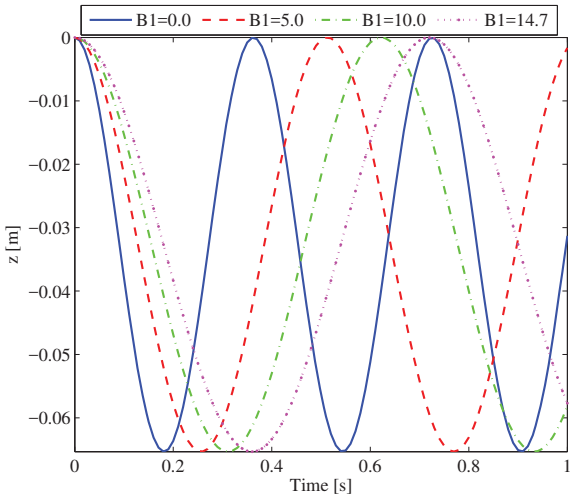

Fig. 6. Telescopic motions of the model in the translational analysis, showing the effect of changing the inerter parameter B_1

given by Eq. (27) is $T_n = 0.36$ s, where $M_1 = 5$ kg, $K_1 = 1500$ N/m, $D_1 = 0$ N/(m/s), and $B_1 = 0$ N/(m/s^2) (the Normal condition). This motion is defined as the normal motion. We then doubled the natural period of the normal motion.

To increase the natural period, we increased the mass of the robot to $M_1 = 19.7$ kg, maintaining $K_1 = 1500$ N/m, $D_1 = 0$ N/(m/s), and $B_1 = 0$ N/(m/s^2) (the Mass condition) . Fig. 5 shows the telescopic motions of Eq. (27) over time. Increasing the mass increased the natural period from $0.36\ s$ to $0.72\ s$, but also increased the amplitude of the robot leg. The amplitude is quadruple with respect to that of the normal motion.

We then increased the natural period by decreasing the spring constant of the robot to $K_1 = 380.1$ N/m, maintaining the other parameters as $M_1 = 5$ kg, $D_1 = 0$ N/(m/s), and $B_1 = 0$ N/(m/s^2) (the Spring condition). Although the natural period was double identically, the spring constant quadrupled the amplitude of the robot leg relative to normal motion (see Fig. 5). Therefore, changing the mass or spring affects the amplitude as well as the natural period.

Finally, we increased the natural period by activating the inerter. The parameters were set as $M_1 = 5$ kg, $K_1 = 1500$ N/m, $D_1 = 0$ N/(m/s), and $B_1 = 14.7$ N/(m/s^2) (the Inerter condition). Under this condition, the natural period doubled from $0.36\ s$ to $0.72\ s$, while the amplitude of the robot leg was unchanged from the normal motion.

To assess how the motion depend on the inerter constant, we varied B_1 as 0.0, 5.0, 10.0, and 14.7 N/(m/s^2). The temporal dynamics under the four inerter constants are plotted in Fig. 6. Clearly the natural period monotonically increasing function B_1, whereas the amplitude of the robot leg is constant with respect to B_1.

V. RUNNING ANALYSIS

Finally, we demonstrate the effectiveness of the ineter through numerical simulations. The physical and control parameters in the simulations are listed in Table I and Table II, respectively. The initial values were set as follows: $\theta_1 = 0.30$ rad, $\theta_2 = 0.00$ rad, $l_1 = 0.65$ m, $x_1 = 0.00$ m, $z_1 = 0.00$ m, $\dot{\theta}_1 = 0.00$ rad/s, $\dot{\theta}_2 = 0.00$ rad/s, $\dot{l}_1 = 0.00$ m/s, $\dot{x}_1 = 0.00$ m/s, $\dot{z}_1 = 0.00$ m/s. The slope angle was set to $\phi = 0.008$ rad. Under these conditions, the running converged to 1-periodic running at a speed of 0.89 m/s. To increase the running speed, we increased the natural period of the robot through the inerter. This action should increase the running speed by delaying the LO timing and increasing the step length.

Fig 7, Fig 10, Fig 13 and Fig. 8, Fig 10, Fig 13 plot the running speed and step length, with respect to inerter constant with $K = 1500, 1525, 1550$ N/m, respectively. Speed and SR are monotonically increased with increasing inerter constant. In contrast, changing the inerter constant negligibly affected the step time (Fig. 9, Fig. 12, Fig. 15), respectively.

TABLE I

PHYSICAL PARAMETERS IN THE SIMULATIONS

Symbol	Unit	Value
m_1	kg	0.05
m_2	kg	5.0
l_0	m	0.8
K	N/m	1500
I	kg $\cdot$ m^2	$0.5 \times m_2 \times (0.15)^2$
g	m/s^2	9.8

TABLE II

CONTROL PARAMETERS IN THE SIMULATIONS

Symbol	Value	Symbol	Value
K_{P1}	1.0	K_{D1}	0.1
K_{P2}	-10.0	K_{D2}	-0.5

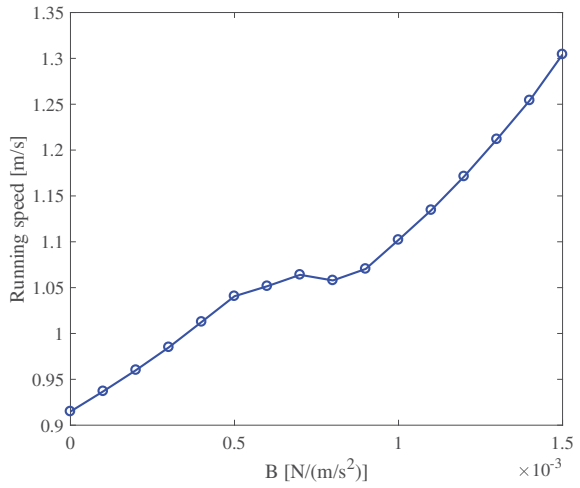

Fig. 7. Running speed with respect to inerter constant B with $K = 1500$

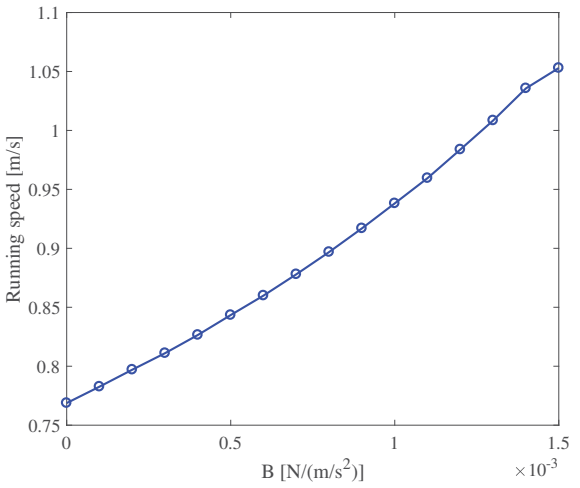

Fig. 10. Running speed with respect to inerter constant B with $K = 1525$

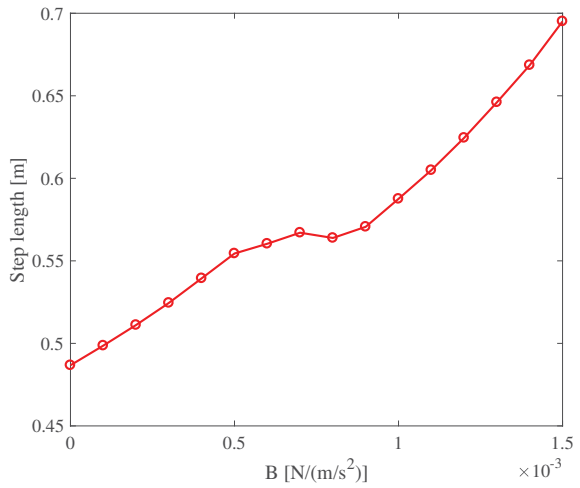

Fig. 8. Step length with respect to inerter constant B with $K = 1500$

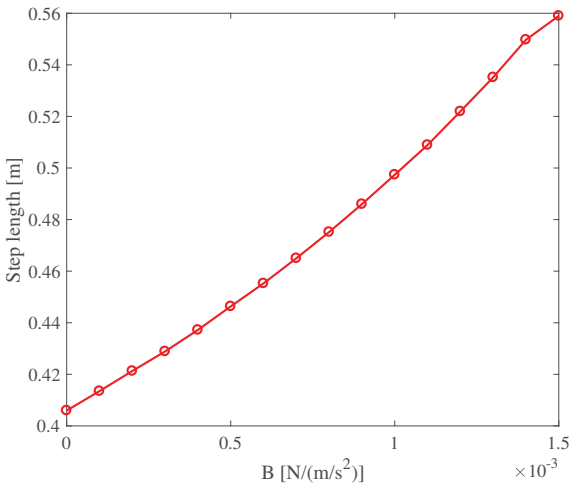

Fig. 11. Step length with respect to inerter constant B with $K = 1525$

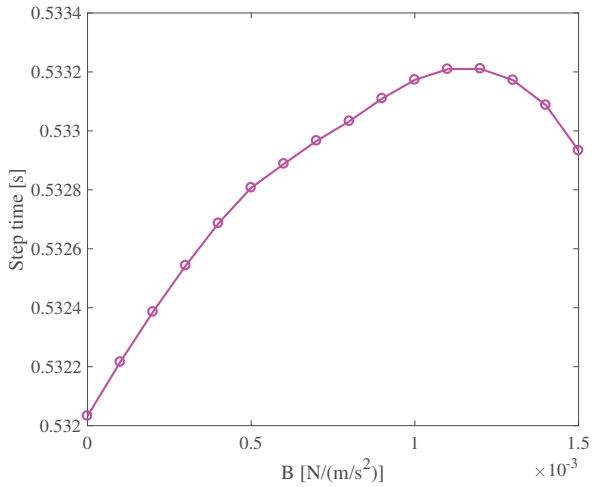

Fig. 9. Step time with respect to inerter constant B with $K = 1500$

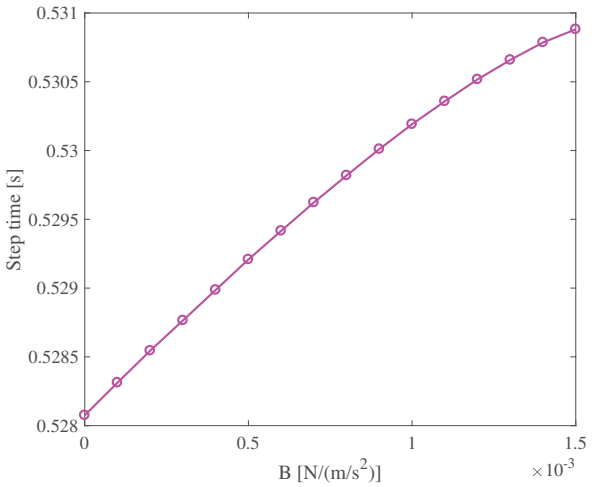

Fig. 12. Step time with respect to inerter constant B with $K = 1525$

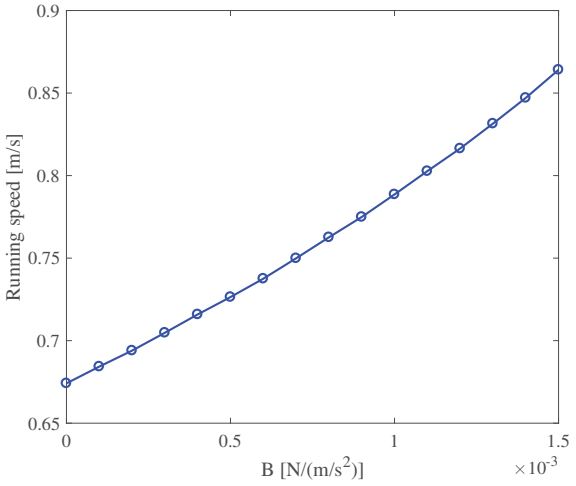

Fig. 13. Running speed with respect to inerter constant B with $K = 1550$

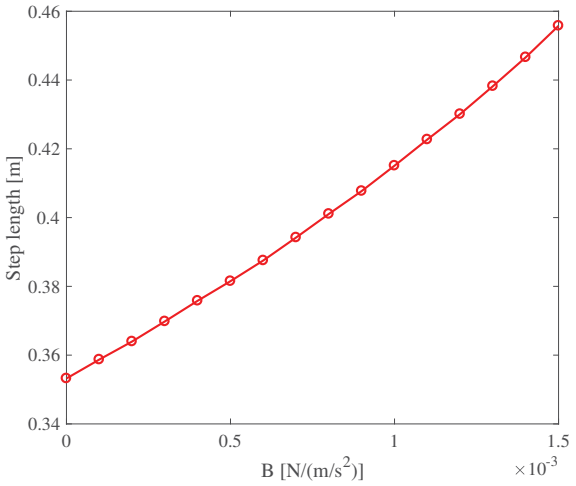

Fig. 14. Step length with respect to inerter constant B with $K = 1550$

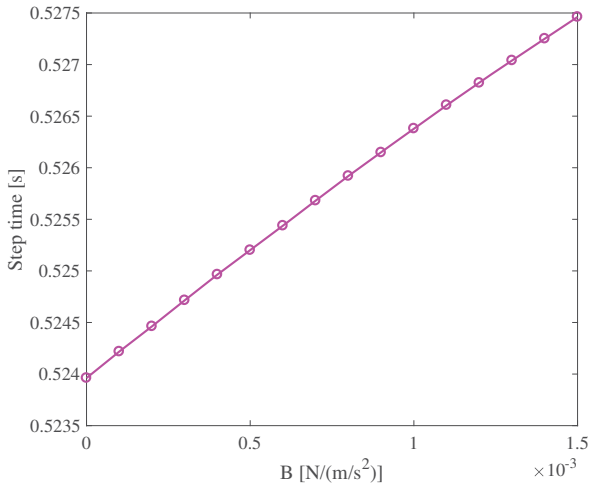

Fig. 15. Step time with respect to inerter constant B with $K = 1550$

VI. CONCLUSION

This paper presents the inerter effects for running robot with mechanical impedance. The property of the inerter were demonstrated in the mathematical analysis. The inerter enables free design of the natural period of the robot, and increases the step length of the model during running. High-speed running of the robot was confirmed in numerical simulations by the inerter effects.

In future work, we will develop an efficient method for designing the spring and inerter in a high-speed running robot. By appropriately setting the spring and inerter constants, we expect to achieve faster running in legged robots with the inerter than in conventional legged robots.

ACKNOWLEDGMENT

This work was supported by JSPS KAKENHI Grant-in-Aid for Young Scientists (B) Grant Number 15K18090.

REFERENCES

[1] HONDA, "Humanoid Robot ASIMO," [Online]. Available: http://www.honda.co.jp/ASIMO/.

[2] PETMAN, "Boston dynamics: Humanoid robot petman," [Online]. Available : http://www.bostondynamics.com.

[3] S. Kajita, K. Kaneko, M. Morisawa, S. Nakaoka, and H. Hirukawa, "Zmp-based biped running enhanced by toe springs," in *Proc. IEEE International Conference on Robotics and Automation (ICRA)*, 2007, pp. 3963–3969.

[4] R. Tajima, D. Honda, and K. Suga, "Fast running experiments involving a humanoid robot," in *Proc. IEEE International Conference on Robotics and Automation (ICRA)*, 2009, pp. 1571–1576.

[5] B. Morris, E. Westervelt, C. Chevallereau, G. Buche, and J. Grizzle, "Achieving bipedal running with rabbit: Six steps toward infinity," in *Fast Motions in Biomechanics and Robotics*. Springer, 2006, pp. 277–297.

[6] K. Nakamura, S. Nakaura, and M. Sampei, "Control of bipedal running by the angular-momentum-based synchronization structure," in *Proc. IEEE International Conference on Robotics and Automation (ICRA)*, 2010, pp. 3310–3315.

[7] P. M. Wensing and D. E. Orin, "High-speed humanoid running through control with a 3d-slip model," in *Proc. IEEE/RSJ International Conference on Intelligent Robots and Systems*, 2013, pp. 5134–5140.

[8] K. Sreenath, H.-W. Park, I. Poulakakis, and J. Grizzle, "Embedding active force control within the compliant hybrid zero dynamics to achieve stable, fast running on mabel," *The International Journal of Robotics Research*, vol. 32, no. 3, pp. 324–345, 2013.

[9] T. Tamada, W. Ikarashi, D. Yoneyama, K. Tanaka, Y. Yamakawa, T. Senoo, and M. Ishikawa, "High-speed Bipedal Robot Running Using High-speed Visual Feedback," in *Proc. IEEE-RAS International Conference on Humanoid Robots (HUMANOIDS)*, 2014, pp. 140–145.

[10] M. Raibert and E. Tello, "Legged robots that balance," *IEEE Expert*, vol. 1, no. 4, pp. 89–89, 1986.

[11] R. Blickhan, "The spring-mass model for running and hopping," *Journal of biomechanics*, vol. 22, no. 11-12, pp. 1217–1227, 1989.

[12] R. Blickhan and R. Full, "Similarity in multilegged locomotion: bouncing like a monopode," *Journal of Comparative Physiology A*, vol. 173, no. 5, pp. 509–517, 1993.

[13] U. Saranlı, Ö. Arslan, M. M. Ankaralı, and Ö. Morgül, "Approximate analytic solutions to non-symmetric stance trajectories of the passive spring-loaded inverted pendulum with damping," *Nonlinear Dynamics*, vol. 62, no. 4, pp. 729–742, 2010.

[14] M. C. Smith, "Synthesis of mechanical networks: The inerter," *IEEE Transactions on Automatic Control*, vol. 47, no. 10, pp. 1648–1662, 2002.

[15] T. McGeer, "Passive dynamic walking," *The International Journal of Robotics Research*, vol. 9, no. 2, pp. 62–82, 1990.

[16] J. W. Grizzle, G. Abba, and F. Plestan, "Asymptotically stable walking for biped robots: Analysis via systems with impulse effects," *IEEE Transactions on Automatic Control*, vol. 46, no. 1, pp. 51–64, 2001.